ORIGINAL ARTICLE

Predictive value of intratumor metabolic and heterogeneity parameters on [18F]FDG PET/CT for EGFR mutations in patients with lung adenocarcinoma

Ming Ni[1,2] · Shicun Wang[2] · Xin Liu[2] · Qin Shi[2] · Xingxing Zhu[2] · Yifan Zhang[2] · Qiang Xie[2] · Weifu Lv[1,3]

Abstract

Purpose This study aimed to investigate the value of metabolic and heterogeneity parameters of 2-deoxy-2[18F]fluoro-D-glucose ([18F]FDG) positron emission tomography/computed tomography (PET/CT) in predicting epidermal growth factor receptor (EGFR) mutations in patients with lung adenocarcinoma (ADC).

Materials and methods A retrospective analysis was performed on 157 patients with lung ADC between September 2015 and June 2021, who had undergone both EGFR mutation testing and [18F]FDG PET/CT examination. Metabolic and heterogeneity parameters were measured and calculated, including maximum diameter (Dmax), maximum standardized uptake value (SUVmax), mean standardized uptake value (SUVmean), metabolic tumor volume (MTV), total lesion glycolysis (TLG), and heterogeneity factor (HF). Relationships between PET/CT parameters and EGFR mutation status were evaluated and a multivariate logistic regression analysis was analyzed to establish a combined prediction model.

Results 108 (68.8%) patients exhibited EGFR mutations. EGFR mutations were more likely to occur in females (51.9% vs. 48.1%, $P = 0.007$), non-smokers (83.3% vs. 16.7%, $P < 0.001$) and right lobes (55.6% vs. 44.4%, $P = 0.017$). High Dmax, MTV and HF and low SUVmean were significantly correlated with EGFR mutations, and the areas under the ROC curve (AUCs) measuring 0.647, 0.701, 0.757, and 0.661, respectively. Multivariate logistic regression analysis suggested that non-smokers (OR = 0.30, $P = 0.034$), low SUVmean (≤ 7.75, OR = 0.63, $P < 0.001$) and high HF (≥ 4.21, OR = 1.80, $P = 0.027$) were independent predictors of EGFR mutations. The AUC of the combined prediction model measured up to 0.863, significantly higher than that of a single parameter.

Conclusions EGFR mutant in lung ADC patients showed more intratumor heterogeneity (HF) than EGFR wild type, which was combined clinical feature (non-smokers), and metabolic parameter (SUVmean) may be helpful in predicting EGFR mutation status, thus playing a guiding role in EGFR-tyrosine kinase inhibitors (EGFR-TKIs) targeted therapies.

Keywords PET/CT · FDG · Lung adenocarcinoma · EGFR · Heterogeneity

✉ Weifu Lv
lwf09@163.com

1 Cheeloo College of Medicine, Shandong University, Jinan 250012, Shandong, China

2 Department of Nuclear Medicine, Division of Life Sciences and Medicine, The First Affiliated Hospital of USTC, University of Science and Technology of China, Hefei 230001, Anhui, China

3 Department of Radiology, Division of Life Sciences and Medicine, The First Affiliated Hospital of USTC, University of Science and Technology of China, Hefei 230001, Anhui, China

Introduction

Lung cancer is the leading cause of cancer-related morbidity and mortality globally [1, 2]. Non-small cell lung cancer (NSCLC) accounts for approximately 85% of all lung cancers and the predominant histologic subtype of NSCLC is adenocarcinoma (ADC) [3]. Mutation in the epidermal growth factor receptor (EGFR) gene, which can promote cell proliferation, differentiation and growth, is one of the most common genomic drivers in lung ADC among the Asian population [4]. EGFR-tyrosine kinase inhibitors (EGFR-TKIs) therapies can prolong 5-year survival rate significantly and have been recommended as the first-line treatment for such patients in advanced NSCLC by clinical

guidelines [5]. Thus, it is crucial to identify EGFR mutation status before individualized targeted therapy is conducted. At present, the tissues for evaluating EGFR mutation status are mainly based on primary tumor tissues, metastasis or body liquid, which may have specimen limitations to prevent some patients from being benefited [6–9]. Therefore, there is an urgent need to find a non-invasive and direct radiographic method for the detection of EGFR mutation status.

It is widely known that NSCLC involves a high heterogeneous group of tumors, manifests itself in different pathological types, stages, gene mutations, and metabolism, with the variety of treatment measures and prognosis proposed [10]. These heterogeneity indexes could be achieved through pathological examination, genetic testing, and clinical evaluation, but also assessed through imaging methods [11]. 2-Deoxy-2[^{18}F] fluoro-D-glucose ([^{18}F]FDG) positron emission tomography/computed tomography (PET/CT) provides unique biological specificity. The time course of radioactivity in tissues reflects the transport of the radiotracer and enzymatic activity, and the radioactivity can be measured over a fixed period at a given time following administration and normalized to yield a standard uptake value (SUV). Differences in properties such as growth rate, vascularity, and necrosis in tumor cells may result in heterogeneous nature of [^{18}F]FDG uptake [12]. Consequently, the parameters measured by [^{18}F]FDG PET/CT maybe associated with the heterogeneity of tumors. Previous studies showed was a valuable tool for assessing functional tumor activity, staging and restaging, evaluating clinical therapeutic effects, and defining the targets for radiotherapy in oncology widely used in NSCLC [13–15].

Recently, one study demonstrated that the EGFR mutation status may alter [^{18}F]FDG uptake via the NADPH oxidase 4 (NOX4)/reactive oxygen species (ROS)/cellular membrane glucose transporter protein 1 (GLUT1) axis [16]. Thus, metabolic parameters of [^{18}F]FDG PET/CT could be thought to predict EGFR mutation status, but the results of related researches remain controversial. For example, some studies had indicated that the maximum standardized uptake values (SUVmax) of the primary lesion was lower [17–19] or higher [20, 21] in EGFR mutations, or showed no significant difference between EGFR mutations and EGFR wild types [22]. In addition, other metabolic parameters in predicting EGFR mutation status, including the mean standardized uptake value (SUVmean), the metabolic tumor volume (MTV) and total lesion glycolysis (TLG), also demonstrated inconsistence in partial researches [23–25].

The coefficient of variance (COV) and heterogeneity factor (HF) acquired by metabolic parameters could also evaluate intratumor heterogeneity, which are known as heterogeneity parameters. COV calculated through SUVmean divided by the standard deviation had already been used to predict EGFR mutation status in NSCLC [25]. HF calculated through linear regressions of MTVs by different SUV thresholds, was already studied in predicting heterogeneity in some solid tumors, such as oral cavity carcinoma, colorectal cancer, pancreatic ductal adenocarcinoma, and uterine leiomyosarcoma gastric cancer [26–30]. Recent studies suggest HF was meaningful in evaluating heterogeneity in terms of occult lymph node metastasis, pathological types, differentiation, T stages and prognosis in NSCLC [31–33], while the correlation between HF and EGFR mutation status in lung ADC patients has never been assessed.

Therefore, the present study aims to analyze the value of metabolic parameters and HF of [^{18}F]FDG PET/CT in predicting the EGFR mutation status in patients with lung ADC before treatments and tries to establish a combined predictive model with clinical and above parameters.

Materials and methods

Patients

We retrospectively analyzed [^{18}F]FDG PET/CT records from patients who had been histologically proven lung ADC between September 2015 and June 2021. This retrospective study was approved by the Ethics Committee of our hospital (2022-RE-074). The inclusion criteria included (1) patients with lung ADC which was confirmed by surgery or histological biopsy in primary lesions, (2) patients who did not receive any therapies before PET/CT scan and EGFR test, and (3) patients who underwent PET/CT scan within one month before surgery or histological biopsy. The exclusion criteria were as follows: (1) genetic mutation status has not been tested; (2) patients with other types of genetic mutations; (3) the volume of lesion was < 1.0 cm^3 or the SUVmax of lesion was ≤ 3.5; (4) patients were detected more than two main lesions in lung or other malignant tumors; and (5) tumor boundary was difficult to delineate due to respiratory movement artifacts, massive pleural effusion, inflammation or atelectasis. Ultimately, 157 patients were enlisted in the study (Fig. 1). Clinical baseline characteristics, including age, sex, smoking history, location, lobe, clinical stage, serum carcinoembryonic antigen (CEA) level and Ki67 index, were collected. The normal level of CEA was 0 ~ 5.0 ng/mL, with Ki67 index ≤ 25% defined as low expression. In this study, smoking status was categorized as a non-smoker or a former/current smoker. A non-smoker was coded as a patient who had smoked fewer than 100 cigarettes during his or her lifetime, the rest defined as a former/current smoker. Clinical staging was based on the 8th edition TNM staging system of NSCLC of the International Association for the Study of Lung Cancer (IASLC) [34].

Fig. 1 The flowchart of patient selection. Others: 7 cases of exon 20 insertion mutation, 3 of exon 21 L861Q mutation, 1 of exon 18 G719X mutation and 4 of co-mutations including exon 18 G917X and exon 20 T790M, exon 21 L861Q and exon 20 T790M, exon 20 S768I and exon 21 L858R, and exon 21 L858R and exon 20 T790M
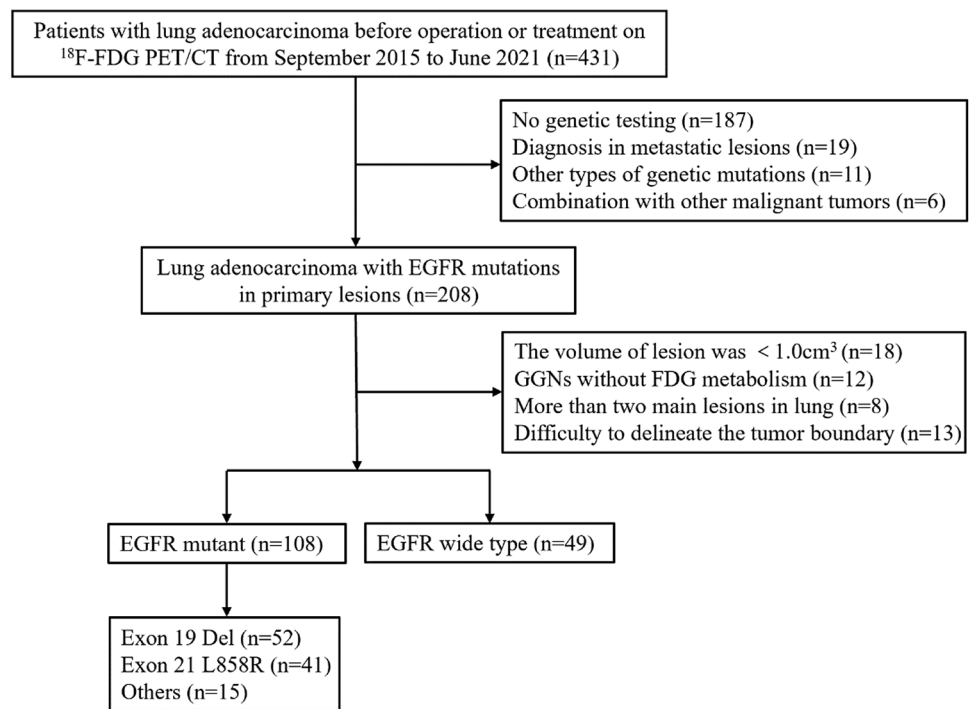
[18F]FDG PET/CT image acquisition

[18F]FDG PET/CT scan was performed on a Biograph 16HR (Siemens Healthcare, Erlangen, Germany). The [18F]FDG was synthesized by Explora FDG4 module, using Eclipse RD cyclotron (Siemens, Germany) in our hospital, and the radiochemical purity of [18F]FDG was > 95%. All patients fasted for 6 ~ 8 h before the PET/CT examination, their serum glucose level less than 11.1 mmol/L. The body was scanned from the skull base to the upper part of the thigh after intravenously injecting [18F]FDG at 3.7 ~ 7.4 MBq/kg and resting approximately for 60 min. The CT scans were performed first (tube voltage, 120 kV; tube current, 100 mAs; pitch, 0.75; slice thickness and spacing, 5 mm; matrix, 512×512; and tube rotation speed, 0.5 s/r). PET scans were then performed with 2 min/bed by a 3D model, a TrueX algorithm (3 iterations, 24 subsets, and 4 mm full width at half maximum) without filtering and smoothing was used to reconstruct the PET images. Attenuation correction of the PET images was performed by means of CT data.

[18F]FDG PET image analysis

One experienced nuclear medicine physician drew boundaries in the axial, coronal, and sagittal PET scans used as the volume of interest (VOI) at a post-processing workstation (Syngo.via, version VB10B, Siemens), which were confirmed by another experienced peer. Both were blinded to clinical and histological results of all patients. The maximum diameter (Dmax) of the primary tumor was measured

at transverse lung window images. The VOI of the primary tumor was delineated to use an iso-contouring tool based on SUVmax, and visually adapted it to cover the entire primary tumor on PET image, but not exceeding the range of the primary tumor. The 40% of SUVmax was served as the threshold to establish VOI to measure the metabolic parameters of the lesion, including SUVmax, SUVmean, MTV, and TLG (Fig. 2a). The parameter of intratumor heterogeneity was represented by HF. The different values of MTV were acquired by three SUVmax thresholds (2.5, 3.0, and 3.5, respectively) automatically in post-processing workstation. The values of MTV were used as the ordinate and SUVmax thresholds (2.5, 3.0, and 3.5) as the abscissa to perform linear regression analysis, the correlation coefficient was thus calculated, and its absolute value was taken as HF (Fig. 2b), which was consistent with previous studies [27, 30].

Detection of histology and EGFR mutations

The histology and EGFR mutational analyses were performed by experienced pathologists at the Department of Pathology in the First Affiliated Hospital of University of Science and Technology of China. The samples were paraffin-embedded tissues acquired through surgical resection, bronchoscopy, or puncture biopsy. The detection kit for human EGFR gene mutations (Wuhan Youzhiyou Medical Technology Co., LTD, China) was used to analyze EGFR mutation status. EGFR exons 18, 19, 20, and 21 were tested by a real-time PCR/amplification refractory mutation system (RT-PCR/ARMS). PCR was
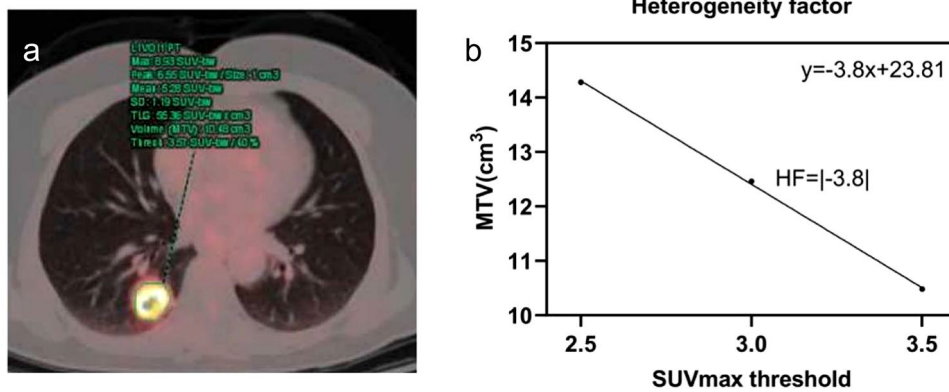
Fig. 2 Process of measuring and calculating metabolic parameters and heterogeneity factor (HF) on [^{18}F]FDG PET/CT. Axial fused PET/CT image (**a**) showed a 56-year-old female with L858R mutation in lung ADC. An iso-contour volume of interest (VOI, green) was automatically drawn with a threshold setting using the 40% of SUVmax, and metabolic parameters, including the mean standardized uptake value (SUVmean), total lesion glycolysis (TLG) and Metabolic tumor volume (MTV), were automatically generated according to the VOI. The values of MTV measured by three SUVmax thresholds (2.5, 3.0, and 3.5, respectively) were 14.28, 12.46, and 10.48, respectively, and linear regression analysis was performed to find the absolute value of the correlation coefficient which was 3.8 (**b**)

performed by PRISM 7500 (Applied Biosystems, Inc. American) real-time fluorescence quantitative PCR.

Statistical analysis

Statistical analysis was performed using SPSS software (version 26.0) and MedCalc software (version 20.106). For each variable, the Shapiro Wilk was used to test the normal distribution. Continuous data were represented by mean ± standard deviation (SD) or medians (interquartile ranges) (Qr), and categorical data were expressed as percentages. Chi-squared test, t test, and Mann–Whitney U test were used to compare clinicopathological and PET indicators between an EGFR mutant and an EGFR wild type. The optimal threshold of each PET parameter that best predicted EGFR mutation status was obtained using the receiver operating characteristic (ROC), and the area under the curve (AUC) was calculated. The cutoff value for differentiating PET parameter groups was the optimal threshold of each variable. Univariate and multivariate logistic regression was conducted to analyze the predictors of gene mutation, which was then combined with independent predictors to construct a logistic regression model to evaluate the association between clinical and PET-related factors with EGFR mutation, with its AUC calculated. The DeLong test was used to compare the differences between receiver operating characteristic (ROC) curves. A 2-sided P value of less than 0.05 was considered statistically significant.

Results

Patient characteristics in lung ADC

Of the 157 patients, 108 (68.8%) exhibited EGFR mutations, while 49 (31.2%) showed an EGFR wild type. The mean age of the two groups was 60.9 ± 9.8 and 63.9 ± 10.4 years, respectively. Exon 19 deletion (19Del) mutation and exon 21 L858R point mutation were the two major mutation subtypes, accounting for 48.1% (52/108) and 38.0% (41/108), respectively. 15 patients were identified to have other EGFR mutations, including 7 cases of exon 20 insertion mutation, 3 of exon 21 L861Q mutation, 1 of exon 18 G719X mutation and 4 of co-mutations. The clinical characteristics of the patients are summarized in Table 1.

Association between clinical characteristics and EGFR mutations in lung ADC

Table 1 shows statistically significant differences in sex, smoking history, and lobe between the EGFR mutation group and the EGFR wild type group. EGFR mutations were more likely to occur in females (51.9% vs. 48.1%, $P = 0.007$), non-smokers (83.3% vs. 16.7%, $P < 0.001$)

Table 1 Clinical characteristics and PET/CT parameters between EGFR mutant and EGFR wild type in patients with lung ADC

Characteristics	EGFR mutant				EGFR wild type (n = 49)	P^a	P^b
	Total (n = 108)	19Del (n = 52)	L858R (n = 41)	Others (n = 15)			
Age, (years, Mean ± SD)	60.9 ± 9.8	60.5 ± 10.5	62.2 ± 7.9	58.7 ± 12.0	63.9 ± 10.4	0.098	0.329
Sex, n (%)						0.007	0.946
Female	56 (51.9)	25 (48.1)	20 (48.8)	11 (73.3)	14 (28.6)		
Male	52 (48.1)	27 (51.9)	21 (51.2)	4 (26.7)	35 (71.4)		
Smoking history, n (%)						< 0.001	0.976
Non-smoker	90 (83.3)	43 (82.7)	34 (82.9)	13 (86.7)	28 (57.1)		
Current or former smoker	18 (16.7)	9 (17.3)	7 (17.1)	2 (13.3)	21 (42.9)		
Tumor location, n (%)						0.324	0.690
Central	12 (11.1)	5 (9.6)	5 (12.2)	2 (13.3)	3 (6.1)		
Peripheral	96 (88.9)	47 (90.4)	36 (87.8)	13 (86.7)	46 (93.9)		
Lobe, n (%)						0.017	0.418
RL	60 (55.6)	31 (59.6)	21 (51.2)	8 (53.3)	37 (75.5)		
LL	48 (44.4)	21 (40.4)	20 (48.8)	7 (46.7)	12 (24.5)		
T stage, n (%)						0.089	0.295
T1–2	69 (63.9)	30 (73.2)	28 (68.3)	11 (73.3)	38 (77.6)		
T3–4	39 (36.1)	22 (26.8)	13 (31.7)	4 (26.7)	11 (22.4)		
N stage, n (%)						0.561	0.268
N0	41 (38.0)	17 (32.7)	18 (43.9)	6 (40.0)	21 (42.9)		
N1–3	67 (62.0)	35 (63.3)	23 (56.1)	9 (60.0)	28 (57.1)		
M stage, n (%)						0.072	0.596
0	45 (41.7)	20 (38.5)	18 (43.9)	7 (46.7)	28 (57.1)		
1	63 (58.3)	32 (61.5)	23 (56.1)	8 (53.3)	21 (42.9)		
Clinical stage, n (%)						0.716	0.474
I + II	30 (27.8)	13 (25.0)	13 (43.9)	4 (26.7)	15 (30.6)		
III + IV	78 (72.2)	39 (56.1)	28 (56.1)	11 (73.3)	34 (68.4)		
CEA levels, n (%)						0.080	0.729
Normal	35 (32.4)	16 (30.8)	14 (34.1)	5 (33.3)	23 (46.9)		
Abnormal	73 (67.6)	36 (69.2)	27 (65.9)	10 (66.7)	26 (53.1)		
Ki67, n (%)						0.087	0.291
≤25%	60 (55.6)	26 (50)	25 (61.0)	9 (60)	20 (40.8)		
>25%	48 (44.4)	26 (50)	16 (39.0)	6 (40)	29 (59.2)		
PET/CT parameters							
Dmax (cm) M (Median, Qr)	3.88 (3.15, 4.41)	3.75 (2.98, 4.53)	4.02 (3.26, 4.36)	3.69 (3.29, 4.70)	3.12 (2.39, 4.07)	0.003	0.651
SUVmax M (Median, Qr)	10.48 (7.73, 13.20)	10.07 (7.73, 12.95)	11.30 (8.11, 15.68)	9.86 (5.91, 12.95)	11.00 (8.15, 15.25)	0.208	0.460
SUVmean M (Median, Qr)	6.03 (4.74, 7.43)	5.87 (4.84, 7.34)	6.61 (4.75, 8.22)	5.72 (3.80, 7.37)	7.57 (5.26, 9.90)	0.001	0.386
TLG (g) M (Median, Qr)	46.8 (17.13, 83.77)	45.03 (18.27, 91.20)	49.79 (14.68, 78.46)	55.29 (16.95, 94.26)	32.85 (13.25, 63.61)	0.140	0.954
MTV (cm3) M (Median, Qr)	7.75 (4.81, 11.51)	7.51 (4.58, 11.62)	8.01 (4.91, 10.94)	8.27 (4.46, 16.34)	4.54 (2.27, 8.55)	< 0.001	0.874
HF M (Median, Qr)	3.15 (2.14, 4.92)	3.17 (2.06, 5.26)	3.16 (2.27, 4.46)	2.97 (1.90, 5.03)	1.73 (1.08, 2.93)	< 0.001	0.917

EGFR epidermal growth factor receptor; *RL* right lobe; *LL* left lobe; *CEA* carcinoembryonic antigen; *Dmax* maximum diameter; *SUVmax* maximum standardized uptake value; *SUVmean* mean standardized uptake value; *MTV* metabolic tumor volume; *TLG* total lesion glycolysis; *HF* heterogeneity factor; *Qr* interquartile rangers

[a]Denotes the *P* value compared EGFR mutant with EGFR wild type

[b]Denotes the *P* value compared 19Del with L858R

and right lobes (55.6% vs. 44.4%, $P = 0.017$). However, no significant differences were found in age, tumor location, TNM stage, clinical stage, CEA levels, and Ki67 index. In addition, subgroup analysis in EGFR mutations group showed no significant differences found in the above clinical parameters between 19Del and L858R mutations.

Association between PET/CT parameters and EGFR mutations in lung ADC

Dmax, MTV, and HF of primary tumors were higher, but SUVmean was lower in the EGFR mutation group than that in the wild type group (3.88 vs. 3.12, 7.75 vs. 4.54 and 3.15 vs. 1.73, 6.03 vs. 7.57; $P = 0.003$, $P < 0.001$, $P < 0.001$, $P = 0.001$, respectively). Moreover, no significant differences were found in SUVmax and TLG between two groups (Table 1). ROC curve analysis revealed that the cut-off values for Dmax, SUVmean, MTV, and HF were 4.28, 7.75, 10.67, and 4.21, corresponding to AUCs of 0.647, 0.661, 0.701, and 0.757, respectively. Furthermore, PET/CT parameters above were not significantly different in mutant subtype analysis.

Prediction of EGFR mutations by univariate and multivariate analyses

Univariate analysis demonstrated that a significant association between EGFR mutation status and sex, smoking history (non-smokers), lobe, Dmax, SUVmean, MTV, and HF. These factors were incorporated into the multivariate logistic regression analysis, which revealed that non-smoking (OR = 0.30, 95% CI 0.10–0.91, $P = 0.034$), low SUVmean (OR = 0.63, 95% CI 0.50–0.80, $P < 0.001$), and high HF (OR = 1.80, 95% CI 1.07–3.02, $P = 0.027$) were independent predictors of EGFR mutation (Table 2). These three factors were combined to construct a prediction model with AUC up to 0.863 (95% CI: 0.800–0.926, sensitivity: 0.861; specificity: 0.756; accuracy: 0.815). The diagnostic efficacy of the combined prediction model was significantly better than a single parameter when assessed by Delong test ($P < 0.001$) (Table 3 and Fig. 3).

Discussion

It is widely known that EGFR mutations in lung ADC are more likely to occur among Asians, females, and non-smokers [4, 35], which had also been verified in our study. Although there was a significant difference in sex ($P = 0.007$) between EGFR mutation group and EGFR wild type group, the mutation frequency of males in EGFR mutation group was as high as 48.1% (52/108). Additionally, the smokers in EGFR mutation group were all males. Therefore, we figured

that EGFR mutations should be tested in the males and regular smokers, which was the same as PIONEER study in Asian populations [4]. Meanwhile, EGFR mutations were more frequently found in the right lobe of patients with lung ADC. However, other clinical characteristics, including age, tumor location, lobe, TNM stage, clinical stage, CEA levels and Ki67 index, showed no significant differences between the two groups. In a word, the clinical information associated with EGFR mutation in lung ADC was quite limited.

Numerous of researches had demonstrated that [18F]FDG PET/CT could predict EGFR mutation status by detecting the changes in intratumor glucose metabolism. SUVmax is the semi-quantitative parameter most widely used, but it is inconsistent as a predictor of EGFR mutation status [16–22]. Chen L et al. [16] had investigated that the NOX4/ROS/GLUT1 axis played an important role in glucose metabolism, and they found ROS activity was reduced when NOX4 expression was downregulated in EGFR mutated cell lines, leading to decreased GLUT1 expression, which explained the reason why SUVmax values were significantly lower in EGFR mutation group in NSCLC. Hong IK et al. [19] also observed the proportion of tumors in advanced ADC patients with low SUVmax (< 9.6) was significantly higher in the EGFR mutated group than that in the EGFR wild type group in lung ADC. However, other studies demonstrated that high SUVmax was positively correlated with EGFR mutation status [20, 21].

In addition, one recent meta-analysis results also showed SUVmax had low pooled sensitivity and specificity in predicting EGFR mutation status in NSCLC, which indicated that [18F]FDG PET/ CT may not be useful for predicting whether there was an EGFR mutation or not [36]. The reason can be that SUVmax only reflects the most active FDG metabolic part of the tumor, but not the whole nature of the tumor. Another important reason for this inconsistency may be related to the pathological subtype of NSCLC. Previous investigations indicated that SUVmax of ADC was lower than squamous cell carcinoma (SCC) [37, 38]. Moreover, the rate of EGFR mutant in ADC was higher than that of SCC as previously described [4]. As a result, the SUVmax may be lower in EGFR mutated group than in the EGFR wild type group in some studies when pathological subtype of NSCLC was not considered. For these reasons, we only selected patients with ADC and did not observe the association between SUVmax and EGFR mutant, similar to the result of a small sample size from the study of Putora PM et al. [39].

However, SUVmean has been identified to reflect more metabolic information than SUVmax [40]. Our study showed that SUVmean was lower in EGFR mutation group than that in EGFR wild type group ($P = 0.001$), which was consistent with previous studies [25, 41]. Therefore, we speculated that SUVmean was the more suitable parameter than SUVmax

Table 2 Univariate and multivariate logistic regression analyses of EGFR mutation in patients with lung ADC

Variables	Univariate		Multivariate	
	OR (95% CI)	P value	OR (95% CI)	P value
Age, (years, mean ± SD)	0.97 (0.94–1.01)	0.102		
Sex				
Female	1.00		1.00	
Male	0.37 (0.18- 0.77)	0.007	0.94 (0.34–2.63)	0.912
Smoking history				
Non-smoker	1.00		1	
Current or former smoker	0.27 (0.13–0.57)	0.001	0.30 (0.10–0.91)	0.034
Tumor location				
Central	1.00			
Peripheral	0.52 (0.14–1.94)	0.331		
Lobe				
RL	1.00		1	
LL	2.47 (1.16–5.24)	0.019	2.52 (0.99–6.39)	0.051
T stage				
T1–2	1			
T3–4	1.95 (0.90–4.25)	0.092		
N stage				
N0	1.00			
N1–3	1.23 (0.62–2.44)	0.561		
M stage				
M0	1.00			
M1	1.87 (0.94–3.70)	0.073		
Clinical stage				
I + II	1.00			
III + IV	1.15 (0.55–2.40)	0.716		
CEA levels (ng/ml)				
< 5.0 (normal)	1.00			
≥ 5.0 (increased)	1.85 (0.93–3.68)	0.082		
Ki67 index				
≤ 25%	1.00			
> 25%	0.60 (0.30–1.19)	0.142		
Parameters of PET				
Dmax (cm)	1.04 (1.01–1.08)	0.012	0.98 (0.92–1.06)	0.659
SUVmax	0.94 (0.87–1.01)	0.070		
SUVmean	0.75 (0.65–0.87)	< 0.001	0.63 (0.50–0.80)	< 0.001
TLG (g)	1.00 (1.00–1.01)	0.223		
MTV (cm³)	1.19 (1.08–1.31)	< 0.001	1.17 (0.93–1.48)	0.185
HF	1.88 (1.26–2.18)	< 0.001	1.80 (1.07–3.02)	0.027

RL right lobe; *LL* left lobe; *CEA* carcinoembryonic antigen; *Dmax* maximum diameter; *SUVmax* maximum standardized uptake value; *SUVmean* mean standardized uptake value; *MTV* metabolic tumor volume; *TLG* total lesion glycolysis; *HF* heterogeneity factor

in reflecting the change of NOX4/ROS/GLUT1 axis with EGFR mutation patients.

MTV represents the volume of metabolically active tumors. We found MTV in the EGFR mutation group was significantly higher than that in the EGFR wild type group (7.75 vs. 4.54, $P < 0.001$). Meanwhile, we also found the maximum diameter of the primary tumor was significantly larger in the EGFR mutant group. Consequently, we speculated the reason may be that the more prominent the tumor size, the more times of division and proliferation, and the greater the probability of random gene mutations in progeny cells, leading to the higher volume of metabolically active tumors [42]. However, MTV could not be considered as an independent predictor to assess EGFR mutation status. TLG

Table 3 Multivariate analysis and combined model for predicting EGFR mutant in patients with lung ADC

Parameters/model	AUC	95% CI	Sensitivity	Specificity	Accuracy
Smoking history	0.631	0.550–0.706	0.833	0.429	0.707
SUVmean	0.661	0.581–0.735	0.815	0.490	0.713
HF	0.757	0.682–0.821	0.852	0.592	0.771
Combined model	0.863	0.800–0.913	0.861	0.756	0.815

SUVmean mean standardized uptake value; *HF* heterogeneity factor; *AUC* area under the curve; *CI* confidence interval
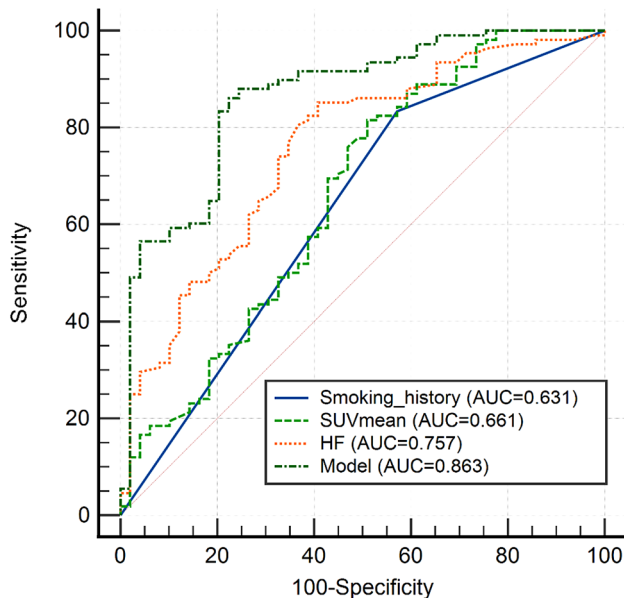
Fig.3 ROC curves of independent predictors and combined prediction models. The predictive value of combined model was 0.863, which was significantly higher than any single parameter through DeLong test

mainly reflects the burden of the whole tumor, calculated by multiplying MTV by SUVmean. Thus, TLG between the two groups did not show a significant difference in our study. However, Yang B et al. [23] pointed out that both MTV and TLG were significantly different between the two groups and MTV could be considered as an independent predictor (ROC = 0.60), which was inconsistent with our study.

In short, the reasons for the inconsistence in predictive capability between these metabolic parameters maybe not only related to different PET scanners, fasting durations, region of interest parameters, and different studies that enrolled in various sample sizes, but also to intratumor heterogeneity. One reasonable explanation for intratumor heterogeneity due to difference in EGFR mutation is that tumor development is a Darwinian evolutionary process, involving the interplay between cancer subclones and the local immune microenvironment [43]. Mutual mutations and evolution between tumor cells cause changes in intratumor heterogeneity. Mao H [44] used a mutant-allele tumor

heterogeneity (MATH) algorithm to measure intratumor heterogeneity and demonstrated that groups with higher MATH values are more likely to be female, smoker and EGFR mutations. We found HF was significantly higher in EGFR mutation group than in EGFR wild type group (3.15 vs. 1.73, $P < 0.001$) in lung ADC. Therefore, we concluded that HF was also a suitable imaging parameter to reflect intratumor heterogeneity, and was positively correlated with gene mutations of tumors. In this study, HF was calculated using the fixed threshold, reflects the heterogeneity of the real metabolic part of the tumor, which had been considered to be better than the percentage threshold method and used in other solid tumors with high FDG uptake [27–30]. Liu X et al. [45] argued that HF calculated by the same method in KRAS mutant was significantly higher than that in wild type patients with colorectal cancer.

Univariate analysis showed that sex, smoking history, lobe, Dmax, SUVmean, MTV, and HF were correlated with EGFR mutation. However, multivariate logistic regression analysis showed that only non-smokers, low SUVmean (≤ 7.75) and high HF (≥ 4.21) were independent predictors in distinguishing EGFR mutation status, and the AUC of the combined prediction model was 0.863, which indicated the discrimination capability was significantly improved with the combination of clinical characteristic and PET parameters. In addition, stratified analysis was performed according to specific EGFR mutation subtypes and the results showed that there were no significant differences among all parameters between 19Del and L858R mutations, consistent with the former study [25].

To our knowledge, this was the first retrospective study to compare the relationship between HF and EGFR mutation status in lung ADC, with a combined model established to identify EGFR mutation status. However, some limitations should be noted. First, this retrospective study was small in sample size, which may cause selection bias; the analysis between different mutant subtypes required a sufficient number of samples as well. Second, our study did not evaluate lung ADC with low [18F]FDG uptake, including ground glass opacities (GGOs). Target delineation used by a threshold of 40% of SUVmax may lead to inaccurate VOI in tumors with low [18F]FDG uptake. However, the patients excluded from this study may affect the accuracy of the

results. Finally, the combined prediction model has not yet been validated, and the prognosis remains unclear due to the short follow-up time of some patients. Further explorations which consider these deficiencies will be significant in the future.

Conclusions

EGFR mutations in patients with lung ADC are correlated with sex, smoking history, lobe, Dmax, SUVmean, MTV, and HF. Non-smokers, low SUVmean, and high HF are independent predictors of EGFR mutation, and the combination of these three factors may further improve discrimination efficiency, which may be considered as a promising and non-invasive tool to predict EGFR mutation status and guide EGFR-TKI targeted therapy. However, a prospective and large-scale investigation is required to further confirm the current study in the future.

Author contributions WFL conceived of the presented idea. MN wrote the original draft. SCW performed the computations. XL and QS collected data. XXZ synthesized and characterized the probes. YFZ and QX performed manuscript editing. All authors have given approval to the final version of the manuscript.

Declarations

Conflict of interest The authors declare no conflict of interest.

Ethical statement This study was approved by the institutional ethics review board of the First Affiliated Hospital of University of Science and Technology of China (2022-RE-074).

References

1. Zhang Y, Luo G, Etxeberria J, Hao Y. Global patterns and trends in lung cancer incidence: a population-based study. J Thorac Oncol. 2021;16:933–44.
2. Sung H, Ferlay J, Siegel RL, Laversanne M, Soerjomataram I, Jemal A, et al. Global cancer statistics 2020: GLOBOCAN estimates of incidence and mortality worldwide for 36 cancers in 185 countries. CA Cancer J Clin. 2021;71:209–49.
3. Zappa C, Mousa SA. Non-small cell lung cancer: current treatment and future advances. Transl Lung Cancer Res. 2016;5:288–300.
4. Shi Y, Au JS, Thongprasert S, Srinivasan S, Tsai CM, Khoa MT, et al. A prospective, molecular epidemiology study of EGFR mutations in Asian patients with advanced non-small cell lung cancer of adenocarcinoma histology (PIONEER). J Thorac Oncol. 2014;9:154–62.
5. Ettinger DS, Wood DE, Aisner DL, Akerley W, Bauman JR, Bharat A, et al. NCCN guidelines insights: non-small cell lung cancer, Version 2.2021. J Natl Compr Canc Netw. 2021;19:254–66.
6. Pisapia P, Pepe F, Iaccarino A, Sgariglia R, Nacchio M, Conticelli F, et al. Next generation sequencing in cytopathology: focus on non-small cell lung cancer. Front Med. 2021;8:633923.
7. Stiller C, Viktorsson K, Paz Gomero E, Hååg P, Arapi V, Kaminskyy VO, et al. Detection of tumor-associated membrane receptors on extracellular vesicles from non-small cell lung cancer patients via immuno-PCR. Cancers. 2021;13:922.
8. Schluckebier L, Caetnao R, Garay OU, Montenegro GT, Marcelo Custodio M, Aran V, et al. (2020) Cost-effectiveness analysis comparing companion diagnostic tests for EGFR, ALK, and ROS1 versus next-generation sequencing (NGS) in advanced adenocarcinoma lung cancer patients. BMC Cancer. 2020;20:875.
9. Guo K, Shao C, Han L, Liu H, Ma Z, Yang Y, et al. Detection of epidermal growth factor receptor (EGFR) mutations from preoperative circulating tumor DNA (ctDNA) as a prognostic predictor for stage I-III non-small cell lung cancer (NSCLC) patients with baseline tissue EGFR mutations. Trans Lung Cancer Res. 2012;10:3213–25.
10. Xue Y, Hou S, Ji H, Han X. Evolution from genetics to phenotype: reinterpretation of NSCLC plasticity, heterogeneity, and drug resistance. Protein Cell. 2017;8:178–90.
11. Assenlin MC, O'Connor JP, Boellaard R, Thacker NA, Jackson A. Quantifying heterogeneity in human tumours using MRI and PET. Eur J Cancr. 2012;48(4):447–445.
12. Huang B, Chan T, Kwong DL, Chan WKS, Khong PL. Nasopharyngeal carcinoma: investigation of intratumoral heterogeneity with FDG PET/CT. Am J Roentgenol. 2012;199(1):169–74.
13. Shao D, Cheng Y, Yuan ZS, Jiang BY, Wang SX. Value of interim ^{18}F-FDG PET/CT for predicting progression-free survival in stage IIIB/IV EGFR-mutant non-small-cell lung cancer patients with EGFR-TKI therapy. Lung Cancer. 2020;149:137–43.
14. Chardin D, Paquet M, Schiappa R, Darcourt J, Bailleux C, Poudenx M, et al. Baseline metabolic tumor volume as a strong predictive and prognostic biomarker in patients with non-small cell lung cancer treated with PD1 inhibitors: a prospective study. J Immunother Cancer. 2020;8:e000645.
15. Carles M, Fechter T, Radicioni G, Schimek-Jasch T, Adebahr S, Zamboglou C, et al. FDG-PET radiomics for response monitoring in non-small-cell lung cancer treated with radiation therapy. Cancers. 2021;13:814.
16. Chen L, Zhou Y, Tang X, Yang C, Tian Y, Xie R, et al. EGFR mutation decreases FDG uptake in nonsmall cell lung cancer via the NOX4/ROS/GLUT1 axis. Int J Oncol. 2019;54:370–80.
17. Lv Z, Fan J, Xu J, Wu F, Huang Q, Guo M, et al. Value of ^{18}F-FDG PET/CT for predicting EGFR mutations and positive ALK expression in patients with non-small cell lung cancer: a retrospective analysis of 849 Chinese patients. Eur J Nucl Med Mol Imaging. 2018;45:735–50.
18. Gao XC, Wei CH, Zhang RG, Cai Q, He Y, Tong F, et al. ^{18}F-FDG PET/CT SUVmax and serum CEA levels as predictors for EGFR mutation state in Chinese patients with non-small cell lung cancer. Oncol Lett. 2020;20:61.
19. Hong IK, Lee JM, Hwang IK, Paik SS, Kim C, Lee SH. Diagnostic and predictive values of ^{18}F-FDG PET/CT metabolic parameters in *EGFR*-mutated advanced lung adenocarcinoma. Cancer Manag Res. 2020;12:6453–65.
20. Ko KH, Hsu HH, Huang TW, Gao HW, Shen D, Chang WC, et al. Value of ^{18}F-FDG uptake on PET/CT and CEA level to predict epidermal growth factor receptor mutations in pulmonary adenocarcinoma. Eur J Nucl Med Mol Imaging. 2014;41:1889–97.
21. Kanmaz ZD, Aras G, Tuncay E, Bahadır A, Kocatürk C, Yaşar ZA, et al. Contribution of ^{18}Fluorodeoxyglucose positron emission tomography uptake and TTF-1 expression in the evaluation of the EGFR mutation in patients with lung adenocarcinoma. Cancer Biomark. 2016;16:489–98.

22. Lee SM, Bae SK, Jung SJ, Kim CK. FDG uptake in non-small cell lung cancer is not an independent predictor of EGFR or KRAS mutation status: a retrospective analysis of 206 patients. Clin Nucl Med. 2015;40:950–8.

23. Yang B, Wang QG, Lu M, Ge Y, Zheng YJ, Zhu H, et al. Correlations study between ^{18}F-FDG PET/CT metabolic parameters predicting epidermal growth factor receptor mutation status and prognosis in lung adenocarcinoma. Front Oncol. 2019;9:589.

24. Liu A, Han A, Zhu H, Ma L, Huang Y, Li M, et al. The role of metabolic tumor volume (MTV) measured by [18F] FDG PET/CT in predicting EGFR gene mutation status in non-small cell lung cancer. Oncotarget. 2017;8:33736–44.

25. Shi A, Wang J, Wang Y, Guo G, Fan C, Liu J. Predictive value of multiple metabolic and heterogeneity parameters of ^{18}F-FDG PET/CT for EGFR mutations in non-small cell lung cancer. Ann Nucl Med. 2022;36:393–400.

26. Kimura M, Kato I, Ishibashi K, Shibata A, Nishiwaki S, Fukumura M, et al. The prognostic significance of intratumoral heterogeneity of 18F-FDG uptake in patients with oral cavity squamous cell carcinoma. Eur J Radiol. 2019;114:99–104.

27. Liu X, Xiang K, Geng GY, Wang SC, Ni M, Zhang YF, et al. Prognostic value of intratumor metabolic heterogeneity parameters on ^{18}F-FDG PET/CT for patients with colorectal cancer. Contrast Media Mol Imaging. 2022. https://doi.org/10.1155/2022/2586245.

28. Kim YI, Kim YJ, Paeng JC, Cheon GJ, Lee DS, Chung JK, et al. Heterogeneity index evaluated by slope of linear regression on ^{18}F-FDG PET/CT as a prognostic marker for predicting tumor recurrence in pancreatic ductal adenocarcinoma. Eur J Nucl Med Mol Imaging. 2017;44:1995–2003.

29. Lee JW, Park JY, Lee HJ, Lee JJ, Moon SH, Kang SY, et al. Preoperative [18F]FDG PET/CT tumour heterogeneity index in patients with uterine leiomyosarcoma: a multicentre retrospective study. Eur J Nucl Med Mol Imaging. 2018;45:1309–16.

30. Liu G, Yin H, Cheng X, Wang Y, Hu Y, Liu T, et al. Intratumor metabolic heterogeneity of gastric cancer on ^{18}F-FDG PETCT indicates patient survival outcomes. Clin Exp Med. 2021;21:129–38.

31. Li R, Lin J, Wang L, Zheng X, Tang K. The association between ^{18}F-fluorodeoxyglucose PET intratumoral metabolic heterogeneity and pathological parameters in non-small cell lung cancer. Nucl Med Commun. 2019;40:1022–8.

32. Ouyang ML, Xia HW, Xu MM, Lin J, Wang LL, Zheng XW, et al. Prediction of occult lymph node metastasis using SUV, volumetric parameters and intratumoral heterogeneity of the primary tumor in T1–2N0M0 lung cancer patients staged by PET/CT. Ann Nucl Med. 2019;33:671–80.

33. Kim DH, Jung JH, Son SH, Kim CY, Hong CM, Ahc BC, et al. Prognostic significance of intratumoral metabolic heterogeneity on ^{18}F-FDG PET/CT in pathological N0 non-small cell lung cancer. Clin Nucl Med. 2015;40(9):708–14.

34. Goldstraw P, Chansky K, Crowley J, Rami-Porta R, Asamura H, Eberhardt WEE, et al. The IASLC lung cancer staging project: proposals for revision of the tnm stage groupings in the forthcoming (eighth) edition of the TNM classification for lung cancer. J Thorac Oncol. 2016;11:39–51.

35. Ha SY, Choi SJ, Cho JH, Choi HJ, Lee J, Jung K, et al. Lung cancer in never-smoker Asian females is driven by oncogenic mutations, most often involving EGFR. Oncotarget. 2015;6:5465–74.

36. Du B, Wang S, Cui Y, Liu G, L X, Li Y. Can ^{18}F-FDG PET/CT predict EGFR status in patients with non-small cell lung cancer? a systematic review and meta-analysis. BMJ Open. 2021;11(6):e044313.

37. Lu P, Yu L, Li Y, Sun Y. A correlation study between maximum standardized uptake values and pathology and clinical staging in nonsmall cell lung cancer. Nucl Med Commun. 2010;37(1):646–51.

38. Takenaka T, Yano T, Ito K, Morodomi Y, Miura N, Marhara Y, et al. Biological significance of the maximum standardized uptake values on positron emission tomography in non-small cell lung cancer. J Surg Oncol. 2009;100(8):688–682.

39. Putora PM, Früh M, Müller J. FDG-PET SUV-max values do not correlate with epidermal growth factor receptor mutation status in lung adenocarcinoma. Respirolgy. 2013;18:734–5.

40. Guo Y, Zhu H, Yao Z, Liu F, Yang D. The diagnostic and predictive efficacy of ^{18}F-FDG PET/CT metabolic parameters for EGFR mutation status in non-small-cell lung cancer: a meta-analysis. Eur J Radiol. 2021;141:109792.

41. Zhu L, Yin G, Chen W, Li X, Yu X, Zhu X, et al. Correlation between EGFR mutation status and F18-fluorodeoxyglucose positron emission tomography computed tomography image features in lung adenocarcinoma. Thorac Cancer. 2019;10:659–64.

42. Marusyk A, Polyak K. Tumor heterogeneity: causes and consequences. Biochim Biophys Acta. 2010;1805:105–17.

43. McGranahan N, Swanton C. Cancer evolution constrained by the immune microenvironment. Cell. 2017;170(5):825–7.

44. Mao H. Clinical relevance of mutant-allele tumor heterogeneity and lung adenocarcinoma. Ann Transl Med. 2019;7(18):432.

45. Liu X, Wang SC, Ni M, Xie Q, Zhang YF, Lv WF, et al. Correlation between ^{18}F-FDG PET/CT intra-tumor metabolic heterogeneity parameters and KRAS mutation in colorectal cancer. Abdom Radiol. 2022;47:1255–64.